Non linear dynamics of Mathieu resonators for resonant gyroscope applications

N.Kacem[12], S.Hentz[1], S.Baguet[2] and R. Dufour[2]
[1]Microsystems Components Laboratory, CEA/LETI - MINATEC, Grenoble, France
[2]LaMCoS, INSA-Lyon, CNRS-UMR5259, 569621, France

For the first time, a complete model describing the non linear dynamics of Mathieu resonators is presented in order to study the stability of resonant MEM gyroscopes.

Introduction:

The resonant sensing technique [1] is highly sensitive, has the potential for large dynamic range, good linearity, low noise and potentially low power. However, when scaling sensors down to NEMS, nonlinearities occur sooner [2] restricting the benefits of the resonant sensors. Moreover, for resonant gyroscopes, the frequency of the Coriolis forces becomes closer to the resonator frequency. The idea is to investigate the dynamic behavior of nonlinear Mathieu resonators [3] in order to find the optimum physical conditions for gyroscope designers to maximise the sensors performances.

Device and equations:

The resonant output gyroscope [4] shown in Figure (1), as its name implies, utilizes resonant sensing as the basis for Coriolis force detection. In its simplest form, the device consists of three resonating elements, a proof mass and two resonating sense elements. The dynamics of the device can be described by a series of coupled differential equations. The proof mass dynamics can be described for most part by a classical spring-mass-damper equation (1). The dynamics of the resonators subjected to an axial time-varying Coriolis force is described by a nonlinear partial differential equation (2) with boundary conditions (3) as follows:

$$\frac{d^2X(t)}{dt^2} + \frac{\delta}{Q}\frac{dX(t)}{dt} + \delta^2 X(t) = \frac{F_e}{M} \qquad \textbf{(1)}$$

$$EI\frac{\partial^4 w(x,t)}{\partial x^4} - \left(N + F_c Cos[\delta t] + \frac{ES}{l}\int_0^l \left[\frac{\partial w(x,t)}{\partial x}\right]^2 dx \right)\frac{\partial^2 w(x,t)}{\partial x^2} + c_R\frac{\partial w(x,t)}{\partial t} + \rho s\frac{\partial^2 w(x,t)}{\partial t^2} = \frac{1}{2}\varepsilon_0\frac{bV^2}{[g - w(x,t)]^2} \qquad \textbf{(2)}$$

$$w(0,t) = \frac{\partial w}{\partial t}(0,t) = w(l,t) = \frac{\partial w}{\partial t}(l,t) = 0 \qquad \textbf{(3)}$$

Model:

The Galerkin discretization procedure was used in order to represent the solution of Equation 2 in terms of a linearly independent set of basis functions $\phi_n(x)$ where each basis function satisfies the boundary conditions described in Equation 3. This procedure permits the transformation of the nonlinear partial differential Equation 2 into a finite system of nonlinear Mathieu equations.

Since we are interested in the response of the resonator at resonance when the first mode is dominant, we reduce the system of ordinary differential equations given by Galerkin discretization to a nonlinear Mathieu equation.

A perturbation technique [5] was used in order to obtain two first order non-linear ordinary-differential equations which describe the amplitude and phase modulation of the response and permits the computation of its stability.

Results:

The effect of the Coriolis force frequency in the resonator frequency response at its primary resonance is shown in Figure (2). We observe the separation of the curve branches when the Coriolis frequency is closed to the resonator frequency. This particular case is treated in Figure (3) for different kinds of resonator behavior. It appears that the quality factor decreases when the angular rate of the microgyroscope increases. Figure (4) shows the effect of the parametric and the nonlinear terms in the periodicity of the resonator response and its amplitude.

Conclusions:

Another limitation for the full scale of a resonant microgyroscope is underlined: the frequency ratio between the proof mass actuation and the resonator sensing. It appears in Figure (5) that the symmetry can be broken between negative and positive Coriolis stress effect when the resonator lose the stability for high coriolis forces amplitude and frequency. The maximum of sensitivity is situated at 0.6 of frequency ratio.

Corresponding author: N. Kacem, CEA/LETI /DRT/DIHS/LCMS, 17 rue des Martyrs 38054 Grenoble, France
Tel: +33-4-38-78-01-27; Fax: +33-4-38-78-51-69; E-mail: najib.kacem@cea.fr

References:

[1] T. Roessig, "IntegratedMEMStuning fork oscillators for sensor applications," Ph.D. dissertation, Department of Mechanical Engineering, University of California, Berkeley, 1998.
[2] Gui, C., Legrenberg, R., Tilmans, H.A., Fluitman, J.H.J., Elwenspoek, M.: "Nonlinearity and hysteresis of resonant strain gauges", J. Microelectromech. Syst. 7, 122–127 (1998)
[3] Barry E. DeMartini, Holly E. Butterfield,, Jeff Moehlis, and Kimberly L. Turner, *Member*, "Chaos for a Microelectromechanical Oscillator Governed by the Nonlinear Mathieu Equation", J. Microelectromech. Syst., Vol. 16, No. 6, December 2007.
[4] Seshia, A.A. ; Howe, R.T.; Montague, S, "An integrated microelectromechanical resonant output gyroscope," Technical Digest Fifteenth IEEE International Conference on Micro Electro Mechanical Systems (MEMS 2002), Las Vegas, NV, p.722-726.
[5] Nayfeh, A.H.: Introduction to Perturbation Techniques. Wiley, New York (1981).

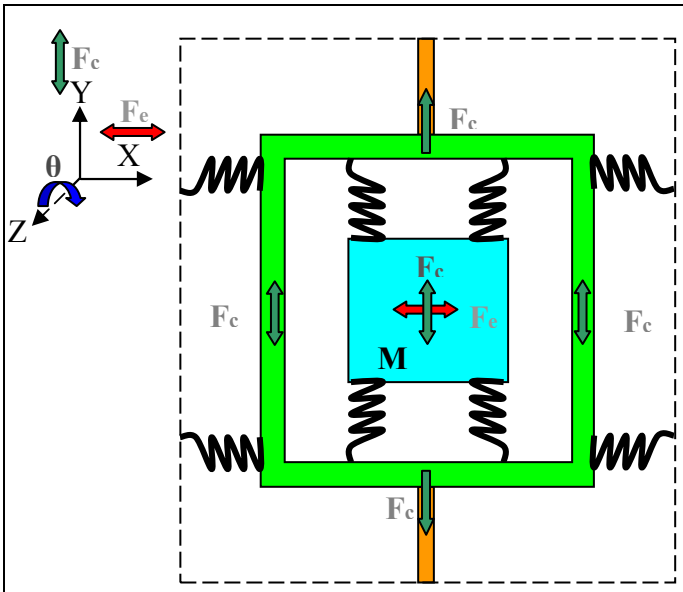

Fig.1: Schema of the resonant microgyroscope.

Resonator design:
Length =50µm
Width = 0.5µm
Thickness = 2µm

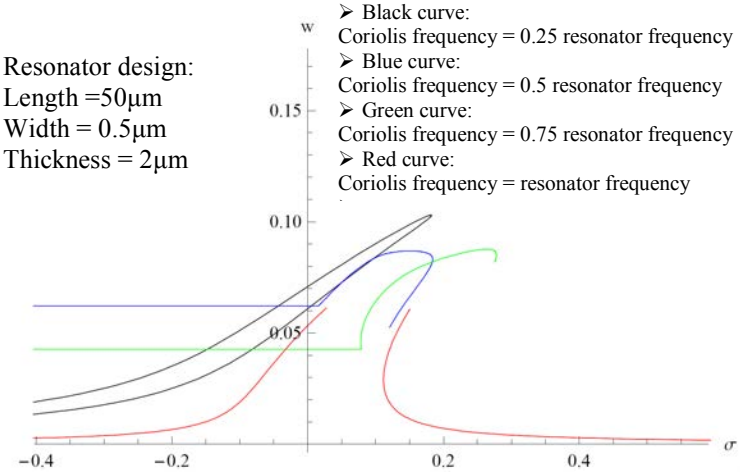

Fig.2: Predicted forced frequency responses including Coriolis force at different frequencies. Microgyroscope angular rate = 150 °/s.

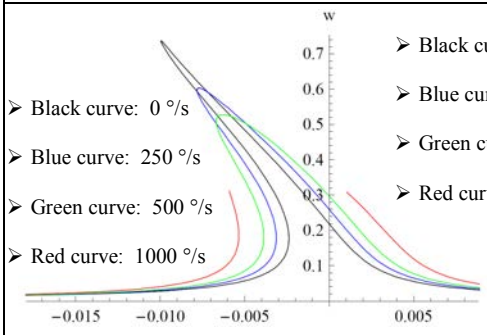

Fig.3.a: Softening behavior

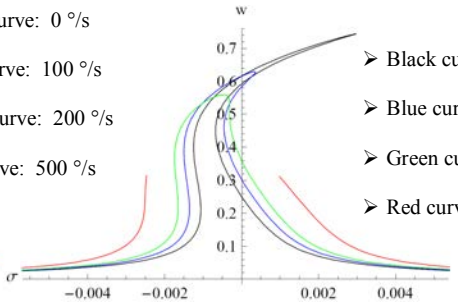

Fig.3.b: Mixed behavior

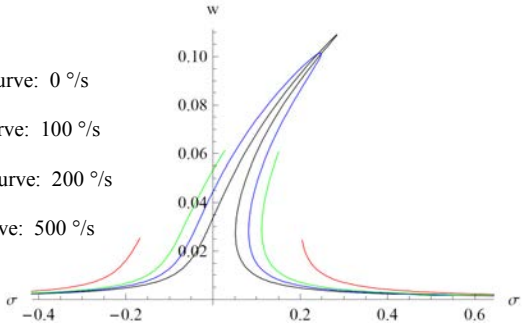

Fig.3.c: Hardening behavior

Resonator design: length =100µm, width = 5µm, thickness = 2µm.	Resonator design: length =50µm, width = 0.5µm, thickness = 2µm.

Fig.3: Predicted forced frequency responses for different angular rates of the resonant microgyrosope at a frequency equal to the resonator frequency with different kinds of behavior. Wmax is the normalized displacement with respect to the gap.

Coriolis frequency = resonator frequency

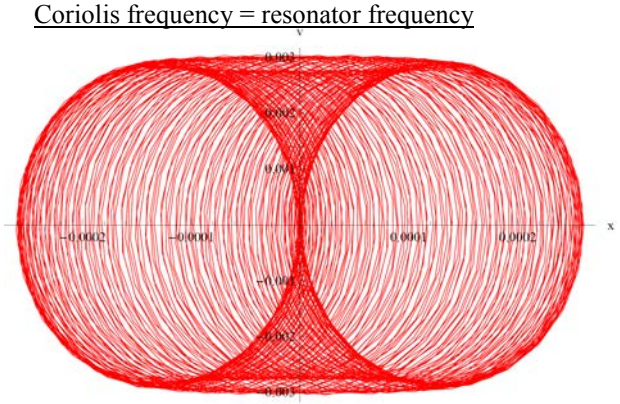

Fig.4.a: Phase plane

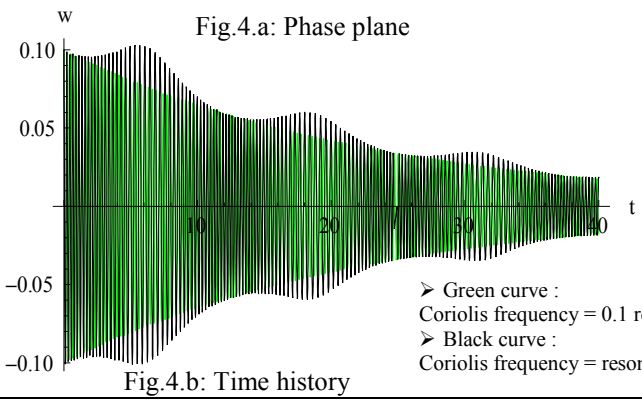

Fig.4.b: Time history

➢ Green curve :
Coriolis frequency = 0.1 resonator frequency
➢ Black curve :
Coriolis frequency = resonator frequency

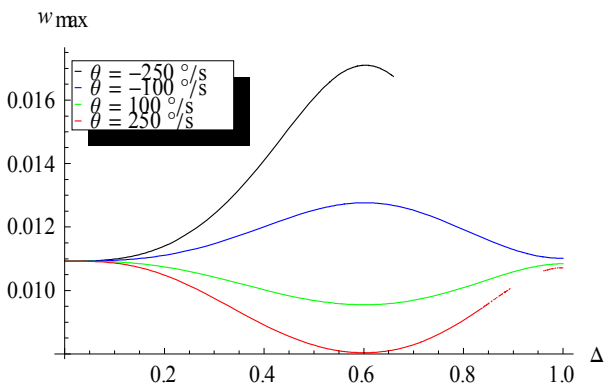

Fig.5 Variation of W_{max} with the frequency ratio between the coriolis force and the sensing resonance. θ is the angular rate of the microgyroscope.

Fig.4: Long time integration
Resonator design: length =50µm,
width = 0.5µm, thickness = 2µm
Microgyroscope angular rate = 1000 °/s